Copper–Sulfur Composite with Carbon-Based Materials for Supercapacitors Applications

Subjects: Chemistry, Applied

Contributor: Junhua Lu, Hedong Jiang, Pingchun Guo, Jiake Li, Hua Zhu, Xueyun Fan, Liqun Huang, Jian Sun, Yanxiang Wang

Supercapacitors (SCs) are a novel type of energy storage device that exhibit features such as a short charging time, a long service life, excellent temperature characteristics, energy saving, and environmental protection. The capacitance of SCs depends on the electrode materials. Currently, carbon-based materials, transition metal oxides/hydroxides, and conductive polymers are widely used as electrode materials. However, the low specific capacitance of carbon-based materials, high cost of transition metal oxides/hydroxides, and poor cycling performance of conductive polymers as electrodes limit their applications. Copper–sulfur compounds used as electrode materials exhibit excellent electrical conductivity, a wide voltage range, high specific capacitance, diverse structures, and abundant copper reserves, and have been widely studied in catalysis, sensors, supercapacitors, solar cells, and other fields.

Keywords: supercapacitors ; electrochemical properties ; specific capacitance ; stability ; copper–sulfur composite ; carbon-based materials ; graphene ; carbon nanotubes ; CC ; acetylene black (AB)

1. Introduction

To cope with the increasingly serious energy shortage, environmental pollution, and other related problems, researchers are vigorously developing green, efficient, and sustainable clean energy. With the rapid development of military equipment, aerospace, rail transit, new energy vehicles, power generation systems, and intelligent electronics, electrochemical energy storage devices have garnered considerable attention in recent years [1][2]. The current energy storage devices mainly include lithium-ion batteries, solid oxide fuel cells, electrostatic capacitors, and supercapacitors. Lithium-ion batteries have the advantages of having a high energy density, long life, low self-discharge rate, etc., and are currently the most common commercially used secondary batteries. However, lithium-ion batteries also have some disadvantages, such as their high cost, environmental sensitivity, and unnecessary heating due to the slow redox process, which can easily lead to thermal runaway and fire [3]. Solid oxide fuel cells offer benefits of being metal-free catalysts, having wide fuel sources, and cogeneration; however, the high reaction temperature of SOFCs leads to high maintenance costs and reduced battery durability over time. Each battery component is exposed to high temperatures, resulting in interface problems that degrade battery performance [4]. The capacitive behavior of electrostatic capacitors refers to the existence of capacitance between electrodes, which involves charging and discharging processes under the action of an electric field. The larger the capacitance, the lesser the power loss. This capacitive effect is generated by the accumulation of charge between the electrodes and does not involve the redox process of electrons and ions. In most batteries, redox reactions often occur, which involve the redox of electrons and ions to produce an electric current. These shortcomings have led researchers to search for electrochemical energy storage systems superior to existing batteries. An SC is an energy storage device based on high-speed electrostatic or Faraday electrochemical processes. **Figure 1** presents the energy density and power density of various energy storage devices [5]. Compared with batteries, supercapacitors (SCs) exhibit a high theoretical energy efficiency of nearly 100%, which is conducive to the application of SC electrochemical devices in power grid load balancing [6]. In addition, SCs are new energy storage devices with a high power density, superior charging/discharging performance, low maintenance cost, safe operation, strong adaptability, good stability, and environmental friendliness, which can shorten the charging time from several hours to several minutes, improve the reliability of renewable power, and reduce waste [7][8][9].

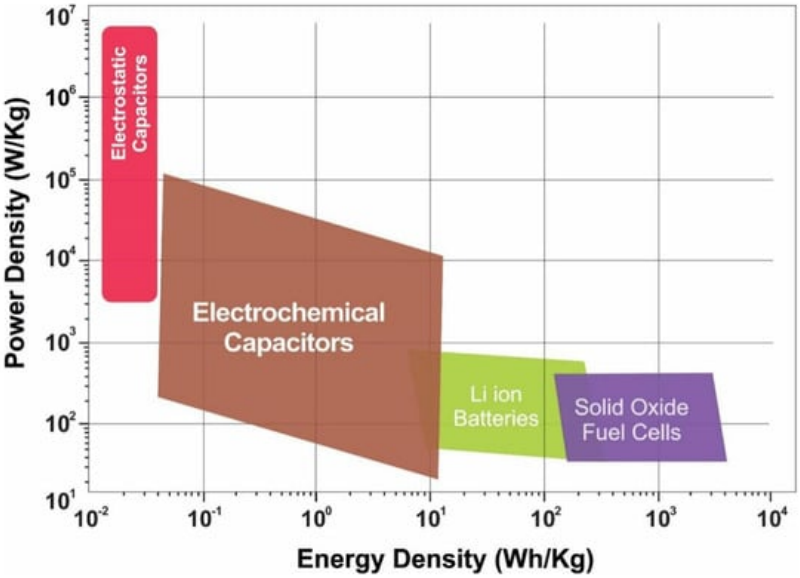

Figure 1. Ragone charts for various energy storage systems, including lithiumiom batteries, solid oxide fuel cells, electrostatic capacitors, and electrochemical capacitors [5].

Electrode materials determine the efficiency of electrochemical energy storage systems, and depending on the energy storage mode, SCs can be divided into double-layer capacitors and pseudocapacitors. Electrode materials used for double-layer capacitors are mainly carbon-based materials (such as graphene) and some two-dimensional materials such as MoS_2. These materials have a high power density; however, compared with pseudocapacitors, the energy density and specific capacitance of double-layer capacitors are low, and graphene sheets are prone to agglomeration, resulting in a decrease in the specific surface area, which eventually reduces the capacity. Graphene is often used as a skeleton material to compound with other materials. MoS_2 has good specific capacitance; however, its electrochemical performance is limited by its inherent secondary agglomeration and low conductivity. In pseudocapacitors, energy is stored through the Faraday redox reaction. At the electrode and electrolyte interface, redox reactions result in higher specific capacitance, energy, and power density [10]. The electrochemical dynamics of pseudocapacitors are capacitive; however, charge storage is achieved through the charge transfer Faraday reaction across the double electric layer. The processes that derive from the Faraday process are fast and reversible surface redox thermodynamics, but capacitance is derived from the linear relationship between the degree of adsorbed charge and the change in potential. Charge storage in pseudocapacitors is generally divided into three types: underpotential deposition occurs at the two-dimensional metal and electrolyte interface, and ions are deposited at the metal interface when the potential is more positive than the corresponding reversible redox potential; redox pseudocapacitance occurs in the Faraday redox system; and in embedded/unembedded pseudocapacitors, ions are embedded in the redox active material but do not undergo crystalline phase transitions during the reaction, that is, their crystal structure does not change. **Figure 2** [11] shows a schematic diagram of the charge storage mechanisms for double-layer capacitors and electrodes of different types of pseudocapacitors. Ther electrode materials used for pseudocapacitors are transition metal oxides, conductive polymers, and transition metal sulfides. Transition metal oxides (e.g., RuO_2 and V_2O_5) have a high theoretical capacity, but poor conductivity leads to their low practical capacity; the voltage window is narrow and can only be applied in aqueous electrolytes [12][13]. The conductive polymer is accompanied by the doping/dedoping of ions during the energy storage process, leading to the repeated entry and exit of ions on the polymer chain, causing the fracture of the molecular chain as well as the generation of irreversible capacity, resulting in poor stability. However, transition metal sulfides have attracted the attention and interest of many researchers because of their low cost, better conductivity than oxides, high theoretical capacity, and especially, their high pseudocapacitance capacity. Currently, transition metal sulfides used in SCs mainly include Cu_xS (x = 1–2), MoS_2, Co_9S_8, NiS, Ni_3S_2, and WS_2 [14]. In 2004, Stevic et al. [15] used copper–sulfur compounds as an electrode material for new SCs and achieved a capacitor capacity as high as 100 F cm^{-2}. Copper–sulfur compounds exhibited a high electronic conductivity, large theoretical specific capacity, excellent redox reversibility, flat voltage plateau, excellent low temperature performance, tunable morphology and composition, rich copper reserves, low resistivity, and a lower electronegativity of sulfur than oxygen. Cu_xS showed significant size-dependent electrochemical properties. Studies have shown that the change in morphology and the reduction in size affect the electrochemical characteristics of pseudocapacitors. Therefore, copper–sulfur compounds have great potential in SCs.

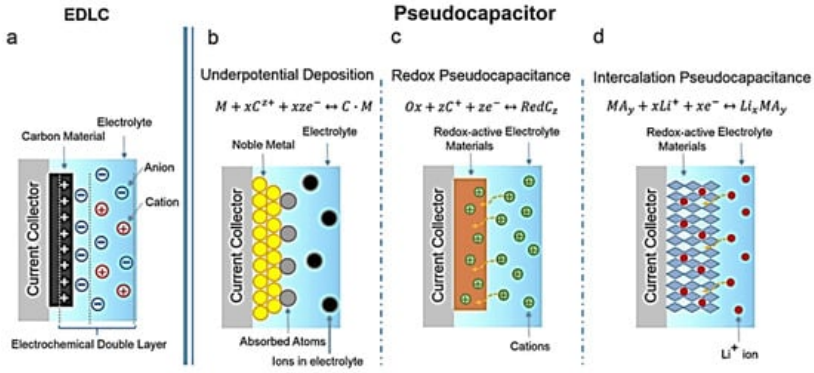

Figure 2. Schematics of charge storage mechanisms for (**a**) an EDLC and (**b**–**d**) different types of pseudocapacitive electrodes: (**b**) underpotential deposition, (**c**) redox pseudocapacitor, and (**d**) ion intercalation pseudocapacitor [11].

Carbon-based materials and their composites, such as graphene, carbon nanotubes, activated carbon, and acetylene black, have attracted considerable research attention in the energy field. These materials exhibit excellent electrochemical performance through the charge storage property of the bilayer behavior and are excellent SC-active electrode materials. Pure copper–sulfur compounds are semiconductors, and their conductivity is lower than those carbon nanomaterials, and compounding copper–sulfur compounds with carbon-based materials can produce more surface active sites to enhance redox reaction efficiency and pseudocapacitance and increase the cycling stability of the capacitor to enhance battery performance [5]. Moreover, the combination of copper–sulfur compounds with carbon-based materials including carbon coating as well as carbon nanotube encapsulation, graphene encapsulation, and core–shell structure formation reduce the agglomeration and cycle life of SCs due to the volume change of copper–sulfur compounds in the constant current charge/discharge process; however, it improves the electrochemical performance of SCs.

2. Copper–Sulfur Composite with Graphene for SC Applications

Graphene exhibits excellent electrical conductivity as well as mechanical properties because of its unique honeycomb structure and large specific surface area (~2630 m^2 g^{-1}) with excellent ion diffusion paths and reduced diffusion resistance. Theoretically, the specific gravity capacitance of single-layer graphene is close to 500 F g^{-1}, and the surface capacitance of its total surface area is 21 µF cm^{-2}. Graphene is oxidized to hydrophilic GO, and the graphite layer spacing is increased from 3.35 Å prior to the oxidation to 7–10 Å after oxidation. The introduction of oxygen atoms in the oxidation process resulted in the formation of a large number of oxygen functional groups, which in turn resulted in a high surface area and many pores; however, the electrical conductivity decreased [16]. By contrast, reduced graphene (rGO) removes the oxygen functional groups and restores the honeycomb two-dimensional structure and high electrical conductivity of graphene. Graphene is typically combined with other materials by using two composite methods, namely surface growth and cladding [17]. Direct growth of a material on the surface of graphene can maintain its high conductivity and two-dimensional properties, which are favorable for electron transport. The preparation process of cladding is simple and can help in achieving a large area coverage, which is suitable for mass production. However, this method affects the two-dimensional properties of graphene and thus deteriorates the electron transport performance.

Currently, CuS is prepared using the hydrothermal method to form copper sulfides on the graphene surface, which controls the specific surface area, copper sulfide morphology (mainly nanosheets, nanorods, quantum dots, hexagonal grains, and nanoparticles), and microstructure of the electrodes to enhance the electrochemical performance of composites. Balu et al. [18] used a hydrothermal method to prepare CuS/GO. Woolly spherical CuS consisting of ultrathin CuS nanosheets uniformly modified on the graphene surface had a specific surface area of 40.3 m^2 g^{-1}, which is nearly twice compared with that of CuS nanospheres (20.8 m^2 g^{-1}). The average pore size of CuS/GO increased from 2.8 nm in the case of CuS nanospheres to 5.1 nm. At a sweep rate of 5 mV s^{-1}, CuS/GO exhibited a specific capacitance of 197.45 F g^{-1} and a capacity retention of 90.35% after 1000 cycles at a current density of 5 A g^{-1}. The unique nanorod structure embedded in the graphene network provides CuS/GO with a mesoporous structure, high surface area, and high electrical conductivity, which enlarges the interfacial area of the nanocomposites, facilitates electron transfer and electrolyte diffusion, and promotes the generation of more active sites in redox reactions to improve the electrochemical performance of SCs. Hout et al. [19] synthesized CuS nanoparticles anchored on rGO nanosheets by using the hydrothermal method. The specific surface area of CuS/rGO was approximately 34.4 m^2 g^{-1} and the volume of the swollen pores was 0.0595 cm^3 g^{-1}. Its specific capacitance reached 587.5 F g^{-1} at a current density of 1 A g^{-1}, and its retention rate was 95% after 2000 cycles at a current density of 10 A g^{-1}. Boopthiraja et al. [20] prepared hexagonal CuS/rGO nanocomposites by using the hydrothermal method in which hexagonal CuS grains were uniformly distributed on the rGO surface. The composite exhibited a large specific surface area of 122 m^2 g^{-1} and pores of size 8–10 nm. The specific capacitance was 1604 F g^{-1}

at a current density of 2 A g^{-1}, and the capacitance was maintained at 97% of the initial level after 5000 cycles. In addition to the hydrothermal method, the composite of graphene and copper–sulfur compounds prepared using successive ionic layer adsorption (SILAR) has been reported. Bulakhe et al. [21] used the SILAR method to modify Cu_2S nanosheets to prepare a nanocomposite Cu_2S/rGO electrode. This nanohybrid exhibited the specific capacitance of 1293 F g^{-1} at a scan rate of 5 mV s^{-1}, which is higher than those of Cu_2S (761 F g^{-1}) and rGO (205 F g^{-1}), with the capacity retention of 94% after 10,000 cycles. Malavekar et al. [22] used the SILAR method to deposit rGO and CuS nanoparticles on a flexible stainless steel substrate in successive layers to obtain CuS/rGO composites with a layered porous structure. The composites have a specific surface area of 77 m^2 g^{-1} and an average pore size of 22 nm. Their specific capacitance reached 1201.8 F g^{-1} at a scan rate of 5 mV s^{-1}, and the capacity was maintained at 98% after 3000 cycles. In the group, composites of copper sulfide compounds and rGO were prepared using the continuous ionic layer adsorption method, which exhibited a specific capacitance of 355.40 F g^{-1} at a current density of 0.5 A g^{-1}.

Graphene-based copper–sulfur compound composites show excellent electrochemical behavior in SC applications; however, they have some drawbacks such as low electrochemical stability. Moreover, the oxidation state of copper is prone to disproportionation under normal experimental conditions, causing complexity of the material composition. Additionally, the surface agglomeration of nanomaterials and the resistance at the electrode–electrolyte interface are high, and a weak bonding force between graphene and metal sulfide nanomaterials leads to electrode shedding and rapid degradation. Sc-related data of copper-sulfur composites and graphene composites are listed in **Table 1**.

Table 1. SC-related data for copper–sulfur composites with graphene composites.

NO.	Electrode Material	Measurement Type	Operating Window (V)	Electrolyte	Energy Storage Performance	Retention Rate	Refs
1	CuS/rGO	Three-electrode	−0.90~0.10	2 M KOH	368.3 F g^{-1} (1 A g^{-1})	88.4% after 1000 cycles	[17]
2	CuS/GO	Two-electrode	0.00~1.00	3 M KOH	197.45 F g^{-1} (5 mV s^{-1})	90.35% after 1000 cycles	[18]
3	CuS/rGO	Three-electrode	0.00~0.40	6 M KOH	587.5 F g^{-1} (1 A g^{-1})	95% after 2000 cycles	[19]
4	CuS/rGO	Three-electrode	0.00~0.50	3 M KOH	1604 F g^{-1} (2 A g^{-1})	97% after 5000 cycles	[20]
5	Cu_2S/rGO	Three-electrode	−1.00~0.00	1 M KOH	1293 F g^{-1} (1 A g^{-1})	94% after 10,000 cycles	[21]
6	CuS/rGO	Three-electrode	−1.10~−0.20	1 M LiClO4	1201.8 F g^{-1} (5 mV s^{-1})	98% after 3000 cycles	[22]
7	CuS/rGO	Three-electrode	−0.20~0.40	6 M KOH	2317.8 F g^{-1} (1 A g^{-1})	96.2% after 1200 cycles	[23]
8	CuS@CQDs-GOH	Three-electrode	−0.10~0.50	6 M KOH	920 F g^{-1} (1 A g^{-1})	90% after 5000 cycles	[24]
9	CuS/GO	Three-electrode	0.00~0.58	3 M KOH	249 F g^{-1} (4 A g^{-1})	95% after 5000 cycles	[25]
10	CuS/rGO	Three-electrode	0.00~0.55	3 M KOH	203 F g^{-1} (0.5 A g^{-1})	90.8% after 10,000 cycles	[26]
11	CuS/CN	Three-electrode	−0.80~1.00	0.1 M Li_2SO_4	379 F g^{-1} (1 A g^{-1})	72.46% after 500 cycles	[27]
12	CuS/GO	Three-electrode	−0.80~−0.15	6 M KOH	497.8 F g^{-1} (0.2 A g^{-1})	91.2% after 2000 cycles	[28]
13	CuS/rGO	Two-electrode	0.00~1.00	6 M KOH	906 F g^{-1} (1 A g^{-1})	89% after 5000 cycles	[29]
14	CuS/rGO	Three-electrode	−0.20~0.60	2 M KOH	1222.5 F g^{-1} (1 A g^{-1})	91.2% after 2000 cycles	[30]
15	CuS/GO	Three-electrode	0.00~0.60	3 M KOH	250 F g^{-1} (0.5 A g^{-1})	70% after 5000 cycles	[31]
16	CuS/rGO	Three-electrode	−1.00~0.00	2 M KOH	3058 F g^{-1} (1 A g^{-1})	60.3% after 1000 cycles	[32]

NO.	Electrode Material	Measurement Type	Operating Window (V)	Electrolyte	Energy Storage Performance	Retention Rate	Refs
17	Cu_2S/rGO	Three-electrode	−0.20~−0.45	3 M KOH	1918.6 F g^{-1} (1 A g^{-1})	95.4% after 5000 cycles	[33]

Note: CuS@CQDs-GOH denotes the complex of carbon-dot-modified CuS with graphene oxide hydrogel; CuS/CN denotes the complex of nitrogen-doped graphene with CuS.

3. Copper–Sulfur Composite with Carbon Nanotubes for SC Applications

Carbon nanotubes (CNTs) have a one-dimensional nanostructure, that is, a hexagonal network of tubular structures bonded by carbon material SP^2. Because of their high electrical conductivity, excellent thermal and mechanical properties, light weight, large surface area, and unique pore structure, they can effectively improve the energy storage capacity and are widely applied for SC-active electrodes. Zhao et al. [34] prepared carbon dot (CQD)-modified CuS/CNTs composites with a three-dimensional grapevine-string-like structure by using the hydrothermal method at 180 °C for 12 h. The diameters of the CuS spheres were in the range 1–2 µm, and the doping of CQDs led to the reduction in the diameter of the CuS spheres to 100–500 nm, which caused the CuS spheres to interact closely with CNTs and accelerated the diffusion of electrons and ions. Their capacitance was 736.1 F g^{-1} at a current density of 1 A g^{-1}, with the capacitance retention of 92% after 5000 cycles. The unique three-dimensional (3D) grapevine structure and the synergistic effect of CuS, CNTs, and CQDs provided additional pseudocapacitance and shortened the diffusion pathway. Quan et al. [35] synthesized 3D porous hierarchical CuS/CNTs@NFs with a flower-like morphology on nickel-foam-based carbon nanotubes by using the solvent-thermal method. CuS/CNTs were uniformly dispersed over the nickel foam surface, and the specific capacitance of 467.02 F g^{-1} was achieved at 0.5 A g^{-1}, which is higher than those of CuS/CNTs (173.84 F g^{-1}) and CuS (163.51 F g^{-1}). The crosslinked structure of the composites provided a fast and easy path for charge transfer while effectively suppressing the self-coiling and agglomeration of CuS nanosheets, which resulted in a higher stability of the composite during the charging and discharging processes.

Improvements in the properties of nanocomposites based on CNTs are attributed to their unique morphology and the synergistic effects of the components, which increase the surface area, thus providing more active sites for electrolyte ions. In addition, CNTs, as the skeleton of highly conductive nanometers, accelerate the charge transfer process and provide a buffer matrix to effectively regulate volume changes under several rapid charge and discharge cycles. However, the current performance of copper–sulfur compound nanocomposites based on CNTs is far lower than the theoretical value, and the agglomeration problem on the surface of nanomaterials adversely affects the electrochemical performance. SC-related data on copper–sulfur composites with carbon nanotubes are listed in **Table 2**.

Table 2. SC-related data on copper–sulfur composites with carbon nanotubes.

NO.	Electrode Material	Measurement Type	Operating Window (V)	Electrolyte	Energy Storage Performance	Retention Rate	Refs
1	CuS/CNTs	Three-electrode	0.00~0.50	3 M KOH	736.1 F g^{-1} (1 A g^{-l})	92% after 5000 cycles	[34]
2	CuS/CNTs	Three-electrode	0.00~0.60	6 M KOH	467.02 F g^{-1} (0.5 A g^{-1})	86% after 5000 cycles	[35]
3	CuS/CNT	Three-electrode	0.00~0.50	2 M KOH	122 F g^{-1} (1.2 A g^{-1})	100% after 1000 cycles	[36]
4	CuS/CNTs	Three-electrode	−0.40~0.60	6 M KOH	2831 F g^{-1} (1 A g^{-1})	90% after 600 cycles	[37]
5	3D-CuS/CNTs	Two-electrode	0.00~0.60	2 M KOH	2204 F g^{-1} (10 mA cm^{-2})	89% after 10,000 cycles	[38]
6	CuS@CNT	Three-electrode	0.00~1.00	2 M KOH	1.51 F cm^{-2} (1.2 A g^{-1})	92% after 1000 cycles	[39]
7	CuS/CNTs	Three-electrode	−0.20~0.60	2 M KOH	566.4 F g^{-1} (1 A g^{-l})	94.5% after 5000 cycles	[40]

4. Copper Sulfide Composite with Activated Carbon in SC

Activated porous carbon (PPAC) has been widely used because of its excellent electrochemical properties, low cost, and large specific surface area [41]. Most of its micropores have diameters between 2 and 50 nm and surface areas up to 3000 m^2 g^{-1}. Li et al. [42] used a solvent-thermal method to homogeneously grow 3D CuS microflora consisting of stacked nanosheets on PPAC. The specific capacitance of the CuS/PPAC electrode was 954.0 F g^{-1} at a current density of 1.0 A g^{-1}, higher than those of pure CuS (579.2 F g^{-1}) and PPAC (329.6 F g^{-1}). The energy density of CuS/PPAC was 47.70 Wh kg^{-1}, which is nearly double that of CuS (29.08 Wh kg^{-1}). The capacitance retention after 5000 charge/discharge cycles was 81.99%, which was higher than that of pure CuS-based electrodes (60.59%). Wang et al. [43] prepared porous CuS/AC with a three-dimensional hollow flower-like structure by using the solvent-thermal method. The specific surface area of the CuS/AC composite was as high as 539.34 m^2 g^{-1} and the pore volume reached 0.22 cm^3 g^{-1}. The high specific surface area and mesoporous structure mitigated the capacity decay because of the volume change during charging and discharging and promoted the diffusion pathways for ionic conductivity and electrolyte penetration, as well as increased the active reaction sites between the electrolyte and electrodes. The introduction of the PPAC layer reduced the electrical resistance from 0.69 Ω for CuS to 0.31 Ω for CuS/AC, which improved the surface contact between CuS and the electrolyte and enhanced diffusion performance. The specific capacitance was 247 F g^{-1} at a current density of 0.5 A g^{-1}, and the capacitance retention was 92% after 5000 cycles.

5. Copper–Sulfur Compounds Compounded with CC in SC

CC is a carbon-based material woven from carbon fibers that exhibits characteristics such as a light weight, low cost, high strength, low density, low thickness, and excellent flexibility. Gong et al. [44] grew CuS on CC in situ through chemical plating, achieving a specific capacity of 1387.1 F g^{-1} at a current density of 2 A g^{-1}, and a capacity retention of 82.9% after 10,000 charge/discharge cycles. Zhou et al. [45] used the solvothermal method to grow dense CuS nanosheets on CC. The staggered ortho-hexagonal CuS nanosheets with suitable channels between them provided abundant electrochemically active sites and facilitated carrier exchange between the electrolyte and electrode interfaces. CuS generated after 4 h of the solvothermal reaction achieved the lowest impedance value (0.84 Ω) and a specific capacity of 436.5 mF cm^{-2} at a current density of 1 mA cm^{-2}, which is higher than those of CC (2.36 mF cm^{-2}), CuS/CC-3 (407.7 mF cm^{-2}), and CuS/CC-5 (430.5 mF cm^{-2}). The capacitance retention of the electrolyte after 5000 charge/discharge cycles was 75.1%. Jin et al. [46] deposited CuS nanosheets on conductive mesoporous CC through electrodeposition. The conductive CC served as both the current carrier and the skeleton of the composite. The g-CuS/CC and p-CuS/CC electrodes were prepared through the constant current and constant potential deposition methods, respectively, with g-CuS/CC achieving a specific surface area of 450.76 m^2 g^{-1}, which was larger than those of p-CuS/CC (397.84 m^2 g^{-1}) and CC (380.46 m^2 g^{-1}). At a current density of 2 mA cm^{-2}, g-CuS/CC exhibited the capacitance of up to 4676 mF cm^{-2}, higher than that of p-CuS/CC (3527 mF cm^{-2}) and 10 times that of CC (490 mF cm^{-2}), with a capacity retention of 89.8% after 10,000 cycles.

The conductive CC acts as a skeleton framework for the electrodeposited composite as well as a collector for the electroactive material. This unique manufacturing process makes the interface extremely smooth while realizing electrochemical double-layer capacitor and pseudocapacitor energy storage, resulting in enhanced electrochemical performance.

6. Copper–Sulfur Composite with Acetylene Black in SC

Acetylene black (AB) is a carbon material produced through the carbonization of acetylene by controlled combustion under pressure in air and has attracted much attention in the field of energy storage because of its light weight, low specific gravity, strong electrolyte absorption ability, chemical stability, low cost, and excellent electrical conductivity [47][48][49]. Huang et al. [50] used the solvothermal method to synthesize AB CuS nanosheet composite CuS/AB with a laminated structure. The intensity ratio of D-band to G-band ID/IG was 1.34, higher than that of pure AB (1.12), resulting in the generation of more defects and vacancies, an increase in the interfacial area between electrolyte/electrode, and enhanced electron transfer. The high conductance of AB and the short ion diffusion paths in the layered CuS nanosheets resulted in a CuS/AB specific capacitance of 2981 F g^{-1} at a current density of 1 A g^{-1}, higher than those of pure CuS nanosheets (920 F g^{-1}) and AB (658 F g^{-1}), and the specific capacitance of the CuS/AB was considerably higher than that of pure AB (1.12). After 600 cycles, the capacity of CuS/AB was maintained at 92%, whereas the CuS and AB electrodes remained at 72.5% and 47.7%, respectively. The specific surface area of pure CuS nanosheets increased from 16.75 m^2 g^{-1} to 62.37 m^2 g^{-1}, which increased the interface area between the electrolyte and electrode. Moreover, the high conductivity of AB and the CuS layer shortened the ion diffusion path and promoted electron transfer. AB anchored on

CuS nanosheets to form a stable three-dimensional structure, reduces deformation, avoids the destruction of electrode materials, and maintains good stability during charge and discharge cycles.

7. MOF-Derived Copper–Sulfur Compound/Carbon-Based Nanocomposites for SC Applications

Metal organic frameworks (MOFs) are three-dimensional inorganic/organic hybrid materials with a periodic network structure formed by the self-assembly of transition metal ions and organic ligands. Generally, with metal ions as the connecting point and organic ligands as a support, MOFs exhibit a large specific surface area, high porosity, low density, tailorability, tunable specific surface area, abundant pores, and structural diversity. MOFs are used as templates for special materials and precursors used to fabricate high porosity. The poor electrical conductivity and cyclic stability of MOF-derived porous materials make it difficult to obtain a high-performance SC when used as electrode materials. Therefore, combining the MOF-derived materials with other materials to form a composite electrode material for improving conductivity, specific capacity, and stability remains challenging. Cu-BTC[$Cu_3(C_9H_3O_6)_2(H_2O)_3]_n$, also known as HKUST-1, is a stable porous MOFs material. Wu et al. [51] used HKUST-1 as a template to prepare carbon-coated $Cu_{1.96}S$ in a single run by using the vulcanization method, which converted 10 nm ultrafine $Cu_{1.96}S$ nanoparticles uniformly embedded in octahedral porous carbon into porous $Cu_{1.96}S$/C composites and maintained the octahedral morphology of MOFs during vulcanization and carbonization. $Cu_{1.96}S$/C exhibits a large specific surface area (140.4 m^2 g^{-1}), which provides more active sites, and it has higher stability than $Cu_{1.96}S$/C at a current density of 0.5 A g^{-1}, a specific capacitance of 200 F g^{-1}, and a capacity retention of 80% after 3000 constant current charge/discharge cycles. Niu et al. [52] prepared flexible composite electrodes, CuS/CNTs, by connecting HKUST-1-derived CuS polyhedra with CNTs. The uniformly distributed CuS polyhedra, consisting of a number of nanorods, had a large specific surface area of 126.4 m^2 g^{-1} and excellent pore size distribution, resulting in a high specific capacity of 606.7 F g^{-1} at 1 A g^{-1}, with the capacitance being 87.0% of the initial value after up to 6000 cycles at 5 A g^{-1}. SC-related data on metal organic skeleton-derived carbon copper sulfide-based nanocomposites are listed in **Table 3**.

Table 3. SC-related data on metal organic skeleton-derived carbon copper sulfide-based nanocomposites.

NO.	Electrode Material	Measurement Type	Operating Window (V)	Electrolyte	Energy Storage Performance	Retention Rate	Refs
1	$Cu_{1.96}S$/C	Two-electrode	0.00~0.90	1 M KOH	200 F g^{-1} (0.5 A g^{-1})	80% after 3000 cycles	[51]
2	CuS/CNTs	Three-electrode	0.00~0.50	6 M KOH	606.7 F g^{-1} (1 A g^{-1})	87.0% after 6000 cycles	[52]
3	$Cu_{1.8}S$/C	Two-electrode	1.00~3.00	1 M $LiPF_6$	740 mAh g^{-1} (50 mA g^{-1})	78% after 200 cycles	[53]
4	Carbon-coated Cu_7S_4	Three-electrode	−0.20~0.70	1 M H_2SO_4	321.9 F g^{-1} (0.5 A g^{-1})	78.1% after 3000 cycles	[54]
5	Cu_9S_8@C-CC@PPy	Three-electrode	−0.40~0.50	1 M KCl	270.72 F g^{-1} (10 mV s^{-1})	83.36% after 3000 cycles	[55]

Note: Cu_9S_8@C-CC@PPy denotes: MOF-derived carbon coated with CuS, followed by deposition of polypyrrole PPy on a carbon cloth substrate using electrochemical deposition.

References

1. Zhong, M.; Zhang, M.; Li, X. Carbon Nanomaterials and Their Composites for Supercapacitors. Carbon Energy 2022, 4, 950–985.
2. Han, Z.; Fang, R.; Chu, D.; Wang, D.-W.; Ostrikov, K. Introduction to Supercapacitors. Nanoscale Adv. 2023, 5, 4015–4017.
3. Winter, M.; Brodd, R.J. What Are Batteries, Fuel Cells, and Supercapacitors? Chem. Rev. 2004, 104, 4245–4270.
4. Vinchhi, P.; Khandla, M.; Chaudhary, K.; Pati, R. Recent Advances on Electrolyte Materials for SOFC: A Review. Inorg. Chem. Commun. 2023, 152, 110724.
5. Samdhyan, K.; Chand, P.; Anand, H.; Saini, S. Development of Carbon-Based Copper Sulfide Nanocomposites for High Energy Supercapacitor Applications: A Comprehensive Review. J. Energy Storage 2022, 46, 103886.

6. Volfkovich, Y.M. Self-Discharge of Supercapacitors: A Review. Russ. J. Electrochem. 2023, 59, 24–36.
7. Anjana, P.M.; Sarath Kumar, S.R.; Rakhi, R.B. Direct Growth of Mn(OH)2/Co(OH)2 Nanocomposite on Carbon Cloth for Flexible Supercapacitor Electrodes. J. Energy Storage 2021, 33, 102151.
8. Wang, F.; Wu, X.; Yuan, X.; Liu, Z.; Zhang, Y.; Fu, L.; Zhu, Y.; Zhou, Q.; Wu, Y.; Huang, W. Latest Advances in Supercapacitors: From New Electrode Materials to Novel Device Designs. Chem. Soc. Rev. 2017, 46, 6816–6854.
9. Iro, Z.S.; Subramani, C.; Dash, S.S. A Brief Review on Electrode Materials for Supercapacitor. Int. J. Electrochem. Sci. 2016, 11, 10628–10643.
10. Xie, J.; Yang, P.; Wang, Y.; Qi, T.; Lei, Y.; Li, C.M. Puzzles and Confusions in Supercapacitor and Battery: Theory and Solutions. J. Power Sources 2018, 401, 213–223.
11. Shao, Y.; El-Kady, M.F.; Sun, J.; Li, Y.; Zhang, Q.; Zhu, M.; Wang, H.; Dunn, B.; Kaner, R.B. Design and Mechanisms of Asymmetric Supercapacitors. Chem. Rev. 2018, 118, 9233–9280.
12. Akinwolemiwa, B.; Wei, C.; Chen, G.Z. Mechanisms and Designs of Asymmetrical Electrochemical Capacitors. Electrochim. Acta 2017, 247, 344–357.
13. Nagaraju, G.; Cha, S.M.; Sekhar, S.C.; Yu, J.S. Metallic Layered Polyester Fabric Enabled Nickel Selenide Nanostructures as Highly Conductive and Binderless Electrode with Superior Energy Storage Performance. Adv. Energy Mater. 2017, 7, 1601362.
14. Shaikh, S.; Rabinal, M.K. Rapid Ambient Growth of Copper Sulfide Microstructures: Binder Free Electrodes for Supercapacitor. J. Energy Storage 2020, 28, 101288.
15. Stevic, Z. Supercapacitors Based on Copper Sulfides. Ph.D. Thesis, University of Belgrade, Belgrade, Serbia, 2004.
16. Stankovich, S.; Dikin, D.A.; Dommett, G.H.B.; Kohlhaas, K.M.; Zimney, E.J.; Stach, E.A.; Piner, R.D.; Nguyen, S.T.; Ruoff, R.S. Graphene-Based Composite Materials. Nature 2006, 442, 282–286.
17. Xiao, W.; Zhou, W.; Feng, T.; Zhang, Y.; Liu, H.; Yu, H.; Tian, L.; Pu, Y. One-Pot Solvothermal Synthesis of Flower-like Copper Sulfide/Reduced Graphene Oxide Composite Superstructures as High-Performance Supercapacitor Electrode Materials. J. Mater. Sci. Mater. Electron. 2017, 28, 5931–5940.
18. Balu, R.; Dakshanamoorthy, A. Synthesis of Wool Ball-like Copper Sulfide Nanospheres Embedded Graphene Nanocomposite as Electrode for High-performance Symmetric Supercapacitor Device. Int. J. Energy Res. 2022, 46, 6730–6744.
19. El-Hout, S.I.; Mohamed, S.G.; Gaber, A.; Attia, S.Y.; Shawky, A.; El-Sheikh, S.M. High Electrochemical Performance of rGO Anchored CuS Nanospheres for Supercapacitor Applications. J. Energy Storage 2021, 34, 102001.
20. BoopathiRaja, R.; Parthibavarman, M.; Prabhu, S.; Ramesh, R. A Facile One Step Hydrothermal Induced Hexagonal Shaped CuS/rGO Nanocomposites for Asymmetric Supercapacitors. Mater. Today Proc. 2020, 26, 3507–3513.
21. Bulakhe, R.N.; Alfantazi, A.; Rok Lee, Y.; Lee, M.; Shim, J.-J. Chemically Synthesized Copper Sulfide Nanoflakes on Reduced Graphene Oxide for Asymmetric Supercapacitors. J. Ind. Eng. Chem. 2021, 101, 423–429.
22. Malavekar, D.B.; Lokhande, V.C.; Mane, V.J.; Kale, S.B.; Bulakhe, R.N.; Patil, U.M.; In, I.; Lokhande, C.D. Facile Synthesis of Layered Reduced Graphene Oxide–Copper Sulfide (rGO-CuS) Hybrid Electrode for All Solid-State Symmetric Supercapacitor. J. Solid State Electrochem. 2020, 24, 2963–2974.
23. Huang, K.-J.; Zhang, J.-Z.; Liu, Y.; Liu, Y.-M. Synthesis of Reduced Graphene Oxide Wrapped-Copper Sulfide Hollow Spheres as Electrode Material for Supercapacitor. Int. J. Hydrog. Energy 2015, 40, 10158–10167.
24. De, B.; Kuila, T.; Kim, N.H.; Lee, J.H. Carbon Dot Stabilized Copper Sulphide Nanoparticles Decorated Graphene Oxide Hydrogel for High Performance Asymmetric Supercapacitor. Carbon 2017, 122, 247–257.
25. Tian, Z.; Dou, H.; Zhang, B.; Fan, W.; Wang, X. Three-Dimensional Graphene Combined with Hierarchical CuS for the Design of Flexible Solid-State Supercapacitors. Electrochim. Acta 2017, 237, 109–118.
26. Cui, Y.; Zhang, J.; Li, G.; Sun, Y.; Zhang, G.; Zheng, W. Ionic Liquid-Assisted Synthesis of rGO Wrapped Three-Dimensional CuS Ordered Nanoerythrocytes with Enhanced Performance for Asymmetric Supercapacitors. Chem. Eng. J. 2017, 325, 424–432.
27. Chen, C.; Zhang, Q.; Ma, T.; Fan, W. Synthesis and Electrochemical Properties of Nitrogen-Doped Graphene/Copper Sulphide Nanocomposite for Supercapacitor. J. Nanosci. Nanotechnol. 2017, 17, 2811–2816.
28. Li, X.; Zhou, K.; Zhou, J.; Shen, J.; Ye, M. CuS Nanoplatelets Arrays Grown on Graphene Nanosheets as Advanced Electrode Materials for Supercapacitor Applications. J. Mater. Sci. Technol. 2018, 34, 2342–2349.
29. Zhao, T.; Yang, W.; Zhao, X.; Peng, X.; Hu, J.; Tang, C.; Li, T. Facile Preparation of Reduced Graphene Oxide/Copper Sulfide Composite as Electrode Materials for Supercapacitors with High Energy Density. Compos. Part B Eng. 2018,

150, 60–67.

30. Zhu, W.; Ou, X.; Lu, Z.; Chen, K.; Ling, Y.; Zhang, H. Enhanced Performance of Hierarchical CuS Clusters Applying TRGO as Conductive Carrier for Supercapacitors. J. Mater. Sci. Mater. Electron. 2019, 30, 5760–5770.
31. Singhal, R.; Thorne, D.; LeMaire, P.K.; Martinez, X.; Zhao, C.; Gupta, R.K.; Uhl, D.; Scanley, E.; Broadbridge, C.C.; Sharma, R.K. Synthesis and Characterization of CuS, CuS/Graphene Oxide Nanocomposite for Supercapacitor Applications. AIP Adv. 2020, 10, 035307.
32. Ghosh, K.; Srivastava, S.K. Enhanced Supercapacitor Performance and Electromagnetic Interference Shielding Effectiveness of CuS Quantum Dots Grown on Reduced Graphene Oxide Sheets. ACS Omega 2021, 6, 4582–4596.
33. Zhuang, G.; Sun, Y.; Chen, X. CuS Cluster Microspheres Anchored on Reduced Graphene Oxide as Electrode Material for Asymmetric Supercapacitors with Outstanding Performance. J. Mater. Sci. Mater. Electron. 2021, 32, 4805–4814.
34. Zhao, T.; Peng, X.; Zhao, X.; Hu, J.; Jiang, T.; Lu, X.; Zhang, H.; Li, T.; Ahmad, I. Preparation and Performance of Carbon Dot Decorated Copper Sulphide/Carbon Nanotubes Hybrid Composite as Supercapacitor Electrode Materials. J. Alloys Compd. 2020, 817, 153057.
35. Quan, Y.; Zhang, M.; Wang, G.; Lu, L.; Wang, Z.; Xu, H.; Liu, S.; Min, Q. 3D Hierarchical Porous CuS Flower-Dispersed CNT Arrays on Nickel Foam as a Binder-Free Electrode for Supercapacitors. New J. Chem. 2019, 43, 10906–10914.
36. Zhu, T.; Xia, B.; Zhou, L.; Lou, X.W.D. Arrays of Ultrafine CuS Nanoneedles Supported on a CNT Backbone for Application in Supercapacitors. J. Mater. Chem. 2012, 22, 7851.
37. Huang, K.-J.; Zhang, J.-Z.; Xing, K. One-Step Synthesis of Layered CuS/Multi-Walled Carbon Nanotube Nanocomposites for Supercapacitor Electrode Material with Ultrahigh Specific Capacitance. Electrochim. Acta 2014, 149, 28–33.
38. Lu, Y.; Liu, X.; Wang, W.; Cheng, J.; Yan, H.; Tang, C.; Kim, J.-K.; Luo, Y. Hierarchical, Porous CuS Microspheres Integrated with Carbon Nanotubes for High-Performance Supercapacitors. Sci. Rep. 2015, 5, 16584.
39. Ravi, S.; Gopi, C.V.V.M.; Kim, H.J. Enhanced Electrochemical Capacitance of Polyimidazole Coated Covellite CuS Dispersed CNT Composite Materials for Application in Supercapacitors. Dalton Trans. 2016, 45, 12362–12371.
40. Hou, X.; Liu, X.; Lu, Y.; Cheng, J.; Luo, R.; Yu, Q.; Wei, X.; Yan, H.; Ji, X.; Kim, J.-K.; et al. Copper Sulfide Nanoneedles on CNT Backbone Composite Electrodes for High-Performance Supercapacitors and Li-S Batteries. J. Solid State Electrochem. 2017, 21, 349–359.
41. González, A.; Goikolea, E.; Barrena, J.A.; Mysyk, R. Review on Supercapacitors: Technologies and Materials. Renew. Sustain. Energy Rev. 2016, 58, 1189–1206.
42. Li, C.; He, P.; Jia, L.; Zhang, X.; Zhang, T.; Dong, F.; He, M.; Wang, S.; Zhou, L.; Yang, T.; et al. Facile Synthesis of 3D CuS Micro-Flowers Grown on Porous Activated Carbon Derived from Pomelo Peel as Electrode for High-Performance Supercapacitors. Electrochim. Acta 2019, 299, 253–261.
43. Wang, G.; Zhang, M.; Lu, L.; Xu, H.; Xiao, Z.; Liu, S.; Gao, S.; Yu, Z. One-Pot Synthesis of CuS Nanoflower-Decorated Active Carbon Layer for High-Performance Asymmetric Supercapacitors. ChemNanoMat 2018, 4, 964–971.
44. Gong, S.-G.; Shi, Y.-H.; Su, Y.; Qi, F.; Song, Y.-H.; Yang, G.-D.; Li, B.; Wu, X.-L.; Zhang, J.-P.; Tong, C.-Y.; et al. Introduction of S-S Bond to Flexible Supercapacitors for High Mass Specific Capacity and Stability. J. Alloys Compd. 2022, 911, 165080.
45. Zhou, W.; Miao, J.; Yan, X.; Li, Y.; Zhu, Y.; Zhang, W.; Zhang, M.; Zhu, W.; Javed, M.S.; Pan, J.; et al. Boosted Electrochemical Performance of CuS Anchored on Carbon Cloth as an Integrated Electrode for Quasi-Solid-State Flexible Supercapacitor. J. Electroanal. Chem. 2021, 897, 115610.
46. Jin, K.; Zhou, M.; Zhao, H.; Zhai, S.; Ge, F.; Zhao, Y.; Cai, Z. Electrodeposited CuS Nanosheets on Carbonized Cotton Fabric as Flexible Supercapacitor Electrode for High Energy Storage. Electrochim. Acta 2019, 295, 668–676.
47. Ahmad, W. P-Type NiO Nanoparticles Enhanced Acetylene Black as Efficient Counter Electrode for Dye-Sensitized Solar Cells. Mater. Res. Bull. 2015, 67, 185–190.
48. Hou, H.; Yang, Y.; Zhu, Y.; Jing, M.; Pan, C.; Fang, L.; Song, W.; Yang, X.; Ji, X. An Electrochemical Study of Sb/Acetylene Black Composite as Anode for Sodium-Ion Batteries. Electrochim. Acta 2014, 146, 328–334.
49. Sun, Y. Synthesis of a Ternary Polyaniline@acetylene Black-Sulfur Material by Continuous Two-Step Liquid Phase for Lithium Sulfur Batteries. Electrochim. Acta 2015, 158, 143–151.
50. Huang, K.-J.; Zhang, J.-Z.; Jia, Y.-L.; Xing, K.; Liu, Y.-M. Acetylene Black Incorporated Layered Copper Sulfide Nanosheets for High-Performance Supercapacitor. J. Alloys Compd. 2015, 641, 119–126.
51. Wu, R.; Wang, D.P.; Kumar, V.; Zhou, K.; Law, A.W.K.; Lee, P.S.; Lou, J.; Chen, Z. MOFs-Derived Copper Sulfides Embedded within Porous Carbon Octahedra for Electrochemical Capacitor Applications. Chem. Commun. 2015, 51,

3109–3112.

52. Niu, H.; Liu, Y.; Mao, B.; Xin, N.; Jia, H.; Shi, W. In-Situ Embedding MOFs-Derived Copper Sulfide Polyhedrons in Carbon Nanotube Networks for Hybrid Supercapacitor with Superior Energy Density. Electrochim. Acta 2020, 329, 135130.
53. Foley, S.; Geaney, H.; Bree, G.; Stokes, K.; Connolly, S.; Zaworotko, M.J.; Ryan, K.M. Copper Sulfide (CuxS) Nanowire-in-Carbon Composites Formed from Direct Sulfurization of the Metal-Organic Framework HKUST-1 and Their Use as Li-Ion Battery Cathodes. Adv. Funct. Mater. 2018, 28, 1800587.
54. Li, L.; Liu, Y.; Han, Y.; Qi, X.; Li, X.; Fan, H.; Meng, L. Metal-Organic Framework-Derived Carbon Coated Copper Sulfide Nanocomposites as a Battery-Type Electrode for Electrochemical Capacitors. Mater. Lett. 2019, 236, 131–134.
55. Liu, Y.-P.; Qi, X.-H.; Li, L.; Zhang, S.-H.; Bi, T. MOF-Derived PPy/Carbon-Coated Copper Sulfide Ceramic Nanocomposite as High-Performance Electrode for Supercapacitor. Ceram. Int. 2019, 45, 17216–17223.